THERMAL ANALYSIS OF MELTING AND FREEZING OF JET AND DIESEL FUELS

C.T. MOYNIHAN *, M.R. SHAHRIARI and T. BARDAKCI

Department of Chemical Engineering and Materials Science, Vitreous State Laboratory, Catholic University of America, Washington, DC 20064 (U.S.A.)

(Received 12 June 1981)

ABSTRACT

The melting and freezing behavior of 16 petroleum fuels and synfuels ranging from jet to diesel have been studied by differential scanning calorimetry (DSC) over the range -60 to $20°C$. None of the fuel samples failed to crystallize on rapid cooling on the DSC, and the degree of supercooling was quite small. Freezing points (f.p.) measured on the DSC at a cooling rate of $10°C$ min^{-1} tended to be a few degrees lower than those measured by ASTM test D 3117-72, as was expected. The shapes of the DSC melting endotherms for $10°C$ min^{-1} heating indicated that more than one crystalline phase freezes out of the fuel on cooling. By selecting the melting point (m.p.) as the temperature halfway down the high temperature side of the last maximum in the DSC melting endotherm, fuel m.p.s measured by DSC were found to agree within experimental error with those measured by ASTM test D 2386-67. M.p.s of fuels can be determined by thermal analysis (DSC or DTA) in well under 10 min, much faster than with the ASTM test. The relative areas under the DSC melting endotherms correlated well with the n-alkane contents of the fuels, suggesting that it is the n-alkanes which initially freeze out.

INTRODUCTION

Meeting future needs for jet aviation fuels may well entail using fuels produced both from alternative sources and from a greater fraction of conventional crudes [1,2]. Such fuels will most likely not meet present jet aviation fuel specifications and, in particular, are apt to freeze at higher temperatures than those currently in use. This has caused a recent resurgence of interest in the freezing behavior of fuels [1-4].

Noel [5,6] found that wax crystallization and melting in lube and fuel oils could readily be characterized by differential scanning calorimetry (DSC) [7]. He also found a good correlation between the onset temperature of crystallization and the temperature of the crystallization peak during cooling on the DSC and, respectively, the ASTM cloud and pour points. (More recently, Noel and Cranton [8] have reviewed applications of thermal analysis to petroleum research.)

---

* Present address: Department of Materials Engineering, Rensselaer Polytechnic Institute, Troy, NY 12181, U.S.A.

In the present paper, we report a DSC study of freezing and melting of sixteen jet or diesel fuels or petroleum distillates intermediate in boiling range between these two types. In particular, we were interested in determining whether DSC (or DTA) could provide a more rapid means of determining the freezing and melting points of fuels than do the standard ASTM tests D 3117-72 [9] and D 2386-67 [10]. ASTM test D 3117-72 for the "wax appearance point of distillate fuels" measures the temperature at which wax crystals first begin to crystallize out of a stirred sample cooled at a rate of about 2°C min^{-1}; in the present paper, we will refer to the results of this test as the ASTM freezing point (f.p.). ASTM test D 2386-67 for the "freezing point of aviation fuels" measures the temperature at which wax crystals disappear (i.e. completely melt or dissolve) when a crystallized sample is stirred and heated at a rate of about 2°C min^{-1}. The term "freezing point" is a misnomer here, and in the present paper we will refer to the results of this test as the ASTM melting point (m.p.).

EXPERIMENTAL

The sixteen fuel samples characterized in this study were obtained from NASA–Lewis Research Center and are briefly described in Table 1. A more complete description of fuels 7, 8, and LFP-1 through LFP-9 is given in Stockemer's report [4]. Fuels X090-205, -206 and -207 are blends of the end member fuels X090-204 and -208. For comparison, we also studied a 25 wt.% n-tridecane– 75 wt.% 1-phenylhexane solution; in the temperature range of our study, only one of these components, the n-tridecane, crystallizes.

The apparatus for ASTM tests D 3117-72 and D 2386-67 differed significantly from the standard apparatus [9,10] only in that the liquid-in-glass thermometer was replaced by a 1/16 in. o.d. stainless steel sheathed copper–constantan thermocouple whose reference junction was kept in an ice–water bath. The thermocouple was calibrated against an NBS-certified Pt resistance thermometer, and its output was monitored with a calibrated digital millivoltmeter. The ASTM f.p. and m.p. were determined in one run by first cooling the sample until it crystallized and then rewarming it to observe the melting. Two determinations on each of two samples (four determinations in all) of the ASTM f.p. and m.p. were done for each fuel; the reproducibility and accuracy were ±0.3°C for both the f.p. and m.p..

DSC studies of melting and freezing were carried out with a Perkin-Elmer Model DSC-2 differential scanning calorimeter cooled by a 2-stage compression refrigerator. Fuel samples, which ranged in mass from 3 to 18 mg, were sealed into Al volatile sample pans. DSC results for a given fuel were independent of sample mass. Two types of DSC scans were carried out. In the first, designed to characterize both freezing and melting behavior, the sample was cooled from 20 to −60°C at a rate of 10°C min^{-1}, held isothermally at −60°C for 1–2 min, and then reheated from −60 to 20°C at 10°C min^{-1}. In the second type of scan, designed to obtain a rapid measurement of the m.p., the sample at 20°C was quenched by programming it to

TABLE 1

Comparison of ASTM and DSC m.p.s and f.p.s

Fuel no.	Type	m.p. (°C)		f.p. (°C)	
		ASTM	DSC	ASTM	DSC
	25 wt.% n-tridecane + 75 wt.% 1-phenylhexane	−27.1	−25.8	−27.1	−31
7	LFP-5 plus 0.1% pour point depressant	−27.6	−28.7	−32.2	−34
8	Shale JP-5	−33.3	−32.7	−35.0	
LFP-1	Paraffinic Jet A (a)	−40.7	−39.7	−43.6	
LFP-3	Paraffinic diesel (b)	−16.5	−16.8	−19.3	−22
LFP-4	Naphthenic diesel	−13.0	−12.5	−19.8	−19
LFP-5	Paraffinic distillate	−28.2	−28.9	−30.5	−35
LFP-6	Naphthenic distillate (c)	−27.9	−28.6	−30.8	−35
LFP-7	Paraffinic diesel (a)	−10.3	−12.8	−14.4	−15
LFP-8	Naphthenic Jet A (c)	−49.8	−51.0	−52.4	
LFP-9	Paraffinic Jet A (b)	−45.1	−44.0	−46.5	
LFP-13	Aromatic distillate	−26.8	−27.4	−30.8	−33
X090-204	Jet A (d)	−43.9	−43.6	−45.9	
X090-205	75 vol.% Jet A (d)	−38.1	−36.8	−40.4	
X090-206	50 vol.% Jet A (d)	−31.3	−31.0	−33.6	−37
X090-207	25 vol.% Jet A (d)	−26.0	−25.7	−28.3	−31
X090-208	Distillate (d)	−22.7	−22.3	−23.9	−27

Fuels followed by the same letter, (a), (b), (c) or (d), are from the same feedstock with different distillation ranges.

cool to −60°C at a nominal rate of 320°C min^{-1}. The sample cannot actually cool at this rate, but takes 4–5 min to reach −60°C. The DSC output was monitored during the quench and, as soon as the crystallization exotherm was passed, the sample was reheated at 10°C min^{-1} to observe the melting behavior.

The DSC temperature scale during heating at 10°C min^{-1} was calibrated by noting the temperature of onset of the melting endotherm of a triply distilled Hg sample (m.p. = −38.9°C). Temperatures measured during 10°C min^{-1} heating are estimated to be accurate to about ±0.5 to 1°C. Calibration of the temperature scale during cooling at 10°C min^{-1} poses something of a problem because of the tendency of even pure samples to supercool through first-order phase transitions. We used the onset temperatures of three phase transitions which tend to exhibit very little supercooling to calibrate the DSC temperature scale during cooling, namely, the freezing point of Hg and the freezing point (−5.4°C) and solid–solid transition point (−18.2°C) of n-tridecane. Indications were that, during cooling at 10°C min^{-1}, the DSC temperature scale between 20 and −40°C read about 3°C low relative to the temperature reading during 10°C min^{-1} heating, and DSC f.p.s given in Table 1 have been corrected upwards by this amount. Even with this correction, temperatures measured above −40°C during 10°C min^{-1} cooling may well be in error by as much as 2°C. Below −40°C during 10°C min^{-1} cooling, the warning light on the DSC indicated that the sample was no longer cooling at the programmed rate, so that temperature readings below this value are not reliable.

RESULTS AND DISCUSSION

DSC freezing and melting curves

In Fig. 1 are shown DSC scans during cooling and subsequent reheating at 10°C min^{-1} of the 25 wt.% n-tridecane–75 wt.% 1-phenylhexane solution and of one of the fuels, LFP-3. The dashed lines in Fig. 1 and subsequent figures are the DSC output during isothermal operation, and the solid lines the output during cooling or heating. The temperature scale during cooling is that obtained from the DSC readout and has not been given the 3°C correction described in the previous section.

During cooling, the onset of crystallization and evolution of the heat of fusion gives rise to an exothermic peak starting at the point marked "f.p." in Fig. 1. On further cooling, more and more of the solid crystallizes from the liquid, as evidenced by continued displacement of the DSC output in the exothermic direction. On reheating, the solid gradually melts (more properly, dissolves) over a range of temperature, giving rise to displacement of the DSC output in the endothermic direction due to absorption of the heat of fusion. This stops at roughly the temperature marked "m.p." in Fig. 1 where melting of the solid phase is complete.

If the fuel sample were close to equilibrium at every temperature during cooling and heating, the DSC freezing and melting curves would be mirror images of one another, and freezing would start and melting finish at the same temperature. The melting and freezing curves in Fig. 1 do, in fact, match quite well several degrees below the f.p., but the initial freezing exotherm is much sharper than the final melting peak. This is because of thermodynamic barriers to crystal nucleation on cooling, which causes the liquid to supercool below the equilibrium f.p. or m.p.
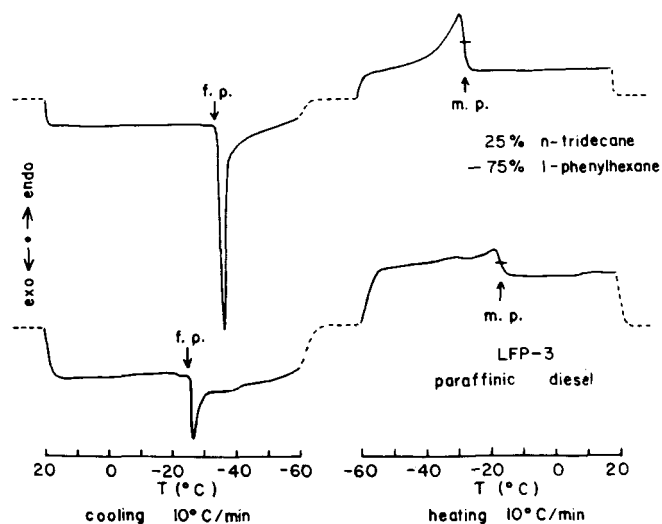

Fig. 1. DSC scans during cooling and subsequent reheating at 10°C min^{-1} of 25 wt.% n-tridecane–75 wt.% 1-phenylhexane solution and LFP-3 diesel fuel.

before crystallization commences. Once crystallization has started, however, it proceeds rapidly, so that a few degrees below the onset of freezing the sample is close to equilibrium with respect to the fraction of solid frozen out. There are no thermodynamic barriers to melting, so that during reheating the sample is close to equilibrium with respect to the fraction of crystalline phase present at all temperatures, and the observed m.p. should be the same as the equilibrium m.p.. (Kinetic barriers can also impede both nucleation and growth of crystals during freezing and dissolution of crystals during melting. These barriers become important, however, only at very high viscosities near the glass transition temperature [6], and the temperature range of our study is well removed from this region.)

In Fig. 2 is shown the DSC output during quenching and subsequent reheating at 10°C min⁻¹ of the LFP-3 fuel. At the start of the quench, the DSC output exhibits a large exothermic transient, after which it recovers gradually as the sample cools toward −60°C. Freezing of the sample shows up as a peak on this recovery curve. The melting endotherm and m.p. observed on reheating are identical to those obtained when the sample is reheated following cooling at 10°C min⁻¹ (compare Figs. 1 and 2). The temperature scale at the bottom of Fig. 2 is for heating at 10°C min⁻¹, while the total time elapsed during quenching and reheating is shown at the top. Note that DSC determination of the melting curve by the method of Fig. 2 can be accomplished in well under 10 min. This is much faster than determination of the ASTM m.p. by test D 2386-67, which generally takes at least 20–30 min.

In Figs. 3–5, 10°C min⁻¹ DSC heating curves taken following a 10°C min⁻¹ cool are shown for the other fuels listed in Table 1. In each case, a melting endotherm is observable.

Comparison of DSC and ASTM m.p.s and f.p.s

The freezing and melting curves shown in Fig. 1 for the 25 wt.% n-tridecane −75 wt.% 1-phenylhexane solution are typical for a binary system in the temperature–composition range where only one component (the n-tridecane) crystallizes from solution. (Since the m.p. is below the solid–solid transition point of n-tridecane (−18.2°C), it is the low temperature crystalline form which freezes out in this case.) It is easily shown from the lever rule [11] for the phase diagram of a simple eutectic binary system that, on heating a partly crystallized sample, the amount of solid melted per degree increases with increasing temperature and is largest right at the liquidus temperature, i.e. the m.p. Hence the DSC melting endotherm should rise with increasing temperature and then fall off vertically at the m.p. The experimental melting curve for the n-tridecane solution in Fig. 3 mimics this expected behavior fairly closely. The main difference is that the experimental melting peak does not drop off vertically at the maximum, but more gradually over about a 2°C range because of the thermal resistance between the sample pan and the DSC pan holder [7]. Neglecting a small correction for this thermal resistance, one would ordinarily take the m.p. of the n-tridecane solution as the temperature at the maximum of the melting endotherm.
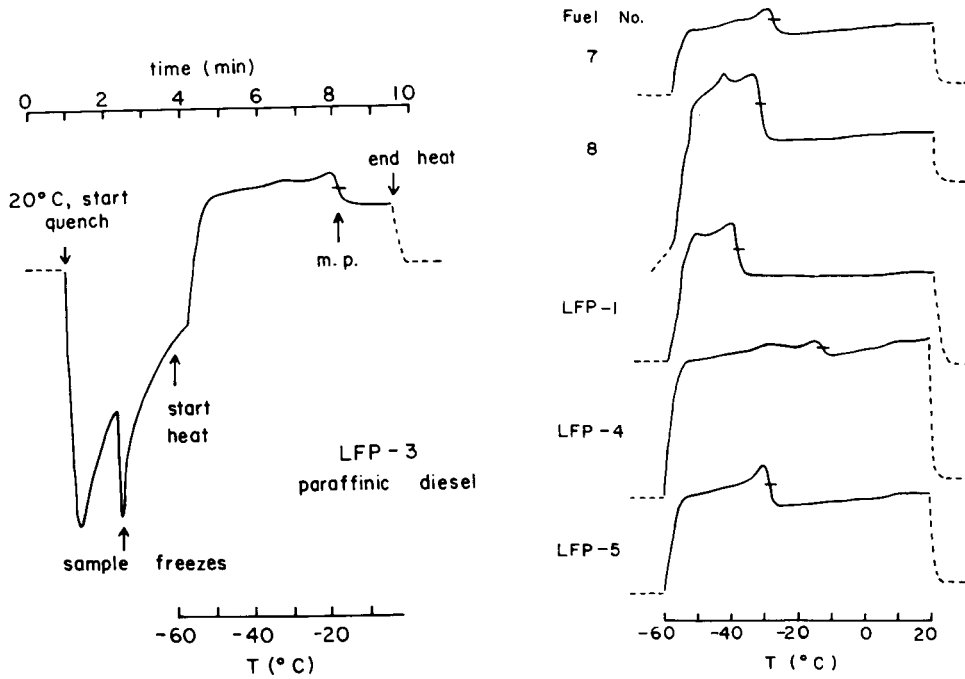
136

Fig. 2. DSC scan during quenching and subsequent reheating at 10°C min⁻¹ of LFP-3 diesel fuel.

Fig. 3. DSC scans of fuels during heating at 10°C min⁻¹ following a 10°C min⁻¹ cool.
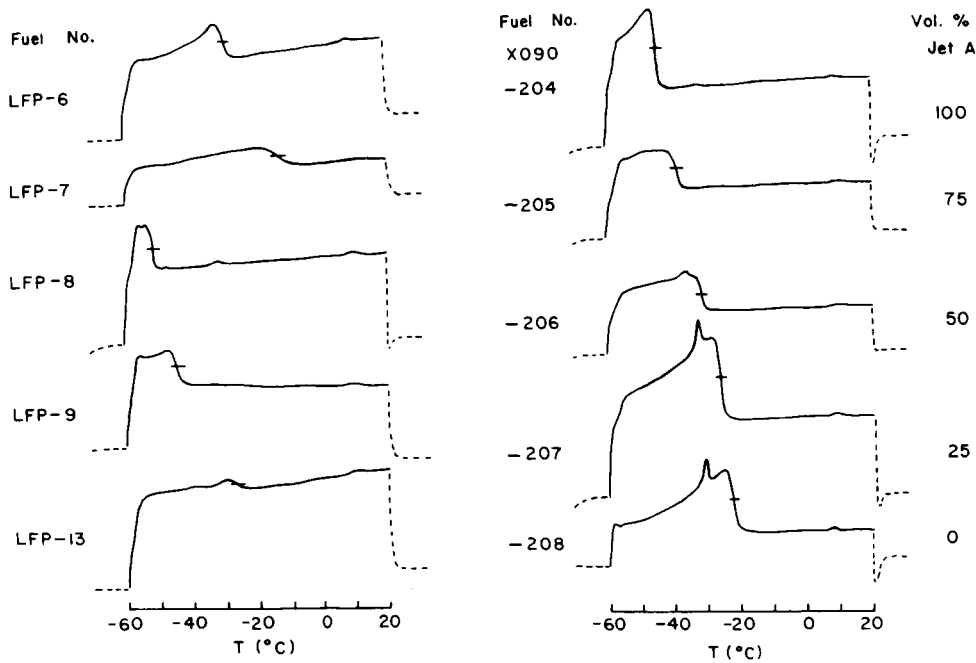
Fig. 4. DSC scans of fuels during heating at 10°C min⁻¹ following a 10°C min⁻¹ cool.

Fig. 5. DSC scans during heating at 10°C min⁻¹ following a 10°C min⁻¹ cool of fuels X090-204 (Jet A), X090-208 (distillate) and blends of these two.

The fuel melting endotherms of Figs. 1–5 are, in general, considerably more complex than that for the n-tridecane solution. In particular, the end of the melting endotherm tends to be smeared out compared with the n-tridecane solution and drops off much more gradually on the high temperature side of the last maximum (cf. especially the scans for LFP-6, LFP-7 and X090-206). Similar behavior was observed by Noel [6] for lube oils and by Zimmerman [12] for fuels. The reason for this is that, in the fuels, many different components (or solid solutions of these) crystallize out on cooling. The observed melting endotherm is thus, to a first approximation, the superposition of the endotherms of a number of different solids, each of which finishes melting at a different temperature. It follows that the final maximum in the melting endotherm for a fuel need not, in general, correspond to the temperature of disappearance of the last crystals, i.e. to the ASTM m.p..

There are thus two factors which tend to smear out the drop off of the fuel melting endotherm at temperatures at and above the final maximum: the thermal resistance between sample pan and DSC pan holder and the superposition of endotherms for a number of solids. Consequently, to choose a m.p. from the DSC scan which correlated well with the ASTM m.p., we had to resort to some empiricism. We found by trial and error that the best agreement was obtained if the DSC m.p. was taken as the temperature halfway down the endotherm on the high temperature side of the last maximum. These temperatures are indicated by a short horizontal line in each of the DSC heating scans of Figs. 1–5.

DSC and ASTM m.p.s for the 16 fuels and the n-tridecane solution are listed in Table 1. The DSC m.p.s are averages of at least four determinations on each fuel and were repeatable to within, typically, $\pm 0.5°C$. The difference between the ASTM and DSC m.p.s is generally of the order of $1°C$ or less, i.e. well within experimental error and considerably less than the reproducibility ($\pm 2.6°C$) considered acceptable for ASTM tests on the same specimen at different laboratories [10]. The largest discrepancy, $2.5°C$, is for fuel LFP-7, whose melting endotherm in the vicinity of the m.p. is, probably not coincidentally, the most smeared out of the samples studied here. It seems safe to conclude that, for hydrocarbon fuels melting below $-10°C$, a DSC (or equivalently, DTA) m.p. determination may be substituted for ASTM test D 2386-67. As noted above, if the method of Fig. 2 is used, the DSC m.p. determination can be carried out much faster than the ASTM test.

ASTM f.p.s for the fuels and the n-tridecane solution are also listed in Table 1 and compared with the DSC f.p.s measured for $10°C$ min^{-1} cooling (cf. Fig. 1). The DSC f.p.s, repeatable to $\pm 0.5°C$, are averages of at least three determinations on each fuel. No DSC f.p.s are listed for fuels freezing below $-40°C$ because of inaccuracies in the DSC temperature scale described above. Because of supercooling, the ASTM f.p. is typically $1-4°C$ lower than the ASTM m.p. The DSC f.p. in turn is typically $2-4°C$ lower than the ASTM f.p. Although this latter discrepancy is barely outside the accuracy of roughly $\pm 2°C$ set for the DSC f.p. by uncertainties in the temperature scale during cooling, it is expected and in the right direction. Near the m.p., thermodynamic barriers to nucleation decrease with decreasing temperature [13], so that a rapidly cooled sample ($10°C$ min^{-1} for the DSC f.p.) will supercool

more than a slowly cooled sample ($\sim 2^\circ$C min^{-1} for the ASTM f.p). Because of supercooling, which will vary in magnitude from fuel to fuel, measurement of the f.p. is not a good characterization method. The interest in these tests is determination of the highest temperature at which a solid phase can exist in equilibrium with the liquid fuel, and this is obtained reliably and with very little additional effort by measuring the m.p.

Correlation of n-alkane content with m.p.s and melting endotherms

For fuels of the types studied here, indications are that the components which freeze out at temperatures near the m.p. are the heavier n-alkanes [3,14]. n-Alkanes have liquid–crystal surface tensions that are unusually low compared with other organic liquids, which in turn leads to unusually low thermodynamic barriers to crystal nucleation [15]. This accounts for the fact that these fuels tend to supercool only a few degrees before freezing and that, to all appearances (viz. the abrupt appearance of a fine cloud of wax crystals throughout the solution during the ASTM f.p. measurement), they nucleate homogeneously rather than heterogeneously. More specifically, it accounts for one of the most significant findings of the present study with regard to the use of DSC for measuring petroleum fuel and synfuel m.p.s, namely that none of the fuels failed to crystallize on rapid cooling of the small DSC sample. In our laboratory we have on occasion studied freezing of hydrocarbon solutions containing no n-alkanes, but with viscosities and m.p.s comparable with those of the present fuels. In many cases, although large samples of these liquids could be induced to crystallize with only moderate difficulty, small samples cooled on the DSC crystallized either not at all or only after extended isothermal holds or thermal cycling below the m.p.

Stockemer [4] has reported the n-alkane contents of several of the fuels studied here and his results are summarized briefly in Table 2. The fuels are listed in order of increasing m.p. As has been noted before [3], the m.p. seems to depend strongly on the heaviest n-alkane present in moderate amount (0.5%), i.e. the heaviest n-alkanes freeze first and melt last, and the m.p. is higher the larger the molecular

TABLE 2

Melting points and n-alkane contents (ref. 4) of fuels

Fuel no.	m.p. (°C)	total % n-alkanes	heaviest and lightest n-alkane present in >0.5%	
LFP-9	−44.0	20.6	$C_{15}H_{32}$	C_9H_{20}
LFP-1	−39.7	26.0	$C_{16}H_{34}$	C_8H_{18}
LFP-5	−28.9	13.9	$C_{17}H_{36}$	$C_{10}H_{22}$
LFP-6	−28.6	12.4	$C_{17}H_{36}$	$C_{11}H_{24}$
LFP-3	−16.8	18.4	$C_{19}H_{40}$	$C_{10}H_{22}$
LFP-7	−12.8	19.6	$C_{19}H_{40}$	$C_{10}H_{22}$
LFP-4	−12.5	8.8	$C_{19}H_{40}$	$C_{11}H_{24}$

weight of the heaviest n-alkane. The relative areas under the melting endotherms correlate well with the total n-alkane contents given in Table 2, e.g. compare the small size of the endotherm for LFP-4 (8.8% n-alkanes) with the large size of the endotherm for LFP-1 (26.0% n-alkanes) in Fig. 3. This correlation is expected if it is indeed primarily the n-alkanes which freeze out near the m.p., since the heats of fusion per gram of the low temperature crystalline forms of the n-alkanes are quite constant in the range $C_{10}H_{22}$ to $C_{16}H_{34}$ [16,17]. It has been suggested [6,12] that the amount of wax crystallized from a fuel or lube oil may be able to be estimated from the area under the melting endotherm.

Structural features in melting endotherms

The melting endotherms of Figs. 1–5 display a variety of shapes. Some, aside from the maximum near the m.p., are fairly featureless (e.g. LFP-6 and LFP-7) and resemble those reported for lube oils by Noel [6]. The majority, however, exhibit secondary structural features in addition to the maximum near the m.p. These sometimes appear as broad shoulders or peaks (e.g. LFP-3 and LFP-4) and sometimes as sharp peaks (e.g. No. 8 and X090-208). This last type of feature was also observed by Zimmerman [12] for a low melting JP-5 fuel. He suggested that the sharp secondary peaks correspond to solid–solid crystalline transitions in the n-alkanes frozen out of solution. This seems unlikely. The solid–solid transitions for the heavier odd-numbered alkanes likely to freeze out of the present fuels (cf. Table 2) occur at temperatures well above the fuel m.p.s [16]. Consequently, these n-alkanes would freeze directly out of the fuel in the low temperature crystalline form and never pass through the solid–solid transition.

Holder and Winkler [18] studied crystallization from dewaxed gas oil of dilute solutions containing two n-alkanes in the range $C_{20}H_{42}$ to $C_{28}H_{58}$. They found that the n-alkanes tended to form ideal solid solutions on freezing if they were close in molecular weight, to form non-ideal solid solutions if there was a moderate difference in molecular weight, and to crystallize independently if there was a large difference in molecular weight. Given the continuous distribution of n-alkanes of different molecular weights which presumably freeze out of the present fuels, it is impossible at present to predict what solid phases form on crystallization, although some solid solution formation seems likely. We have already noted that the smearing out of the melting endotherm near the m.p. indicates the presence of more than one crystalline phase in the frozen fuel; these may well be multicomponent solid solutions of different compositions. It seems likely that the occurrence of secondary peaks in the endotherms is due to the same cause. The secondary peak would then correspond to the disappearance (complete melting) of one of these phases, i.e. to the crossing of a eutectic line in the multicomponent phase diagram [19]. Depending on the number of different crystalline phases in the frozen fuel and the composition differences among them, the disappearance of one of them might or might not give rise to a well-resolved feature on the overall melting endotherm.

M.p.s and melting endotherms of fuel blends

The melting endotherms of the fuel blends of Fig. 5 are interesting in this regard. The two end member fuels, X090-204 and -208, have endotherms with a fairly sharp peak at the m.p.; in addition, the X090-208 endotherm has a sharp secondary peak. Presumably, the molecular weight distribution of different *n*-alkanes in these two fuels is fairly narrow, with the average *n*-alkane molecular weight being larger for the higher melting fuel. The melting endotherms of the blends, especially those for X090-205 and -206, are much more smeared out than those of the end member fuels. This may, in part, reflect the broader *n*-alkane molecular weight distributions in the blends, although concentration changes of each of the *n*-alkanes on blending are no doubt of equal importance. The sharp secondary peak in the X090-208 endotherm shifts to lower temperatures and gradually disappears as this fuel is diluted with X090-204. This behavior is expected if the secondary peak occurs when a eutectic line is crossed, since in multicomponent systems eutectic temperatures are composition dependent.

In Fig. 6, the m.p.s of the blended fuels X090-204 to -208 are plotted against composition. The plot is monotonic, showing that the pseudobinary line representing these blends lies on a single liquidus surface of the multicomponent phase diagram [11]. These surfaces are almost always concave upwards, so that the positive deviations from linearity in Fig. 6 are expected.

Effect of pour point depressant

Fuels 7 and LFP-5 differ only in that fuel 7 contains 0.1% pour point depressant [4]. Pour point depressant inhibits the tendency of wax crystals to grow together, forming a continuous matrix which entraps remaining liquid and gives solid properties to the partly frozen fuel, i.e. the partly frozen fuel will not pour. The mechanism of action of the pour point depressant is not well understood, but one would presume that the depressant molecules are adsorbed at the liquid-crystal interface, lowering the liquid-crystal surface tension and repressing the tendency of small wax crystals to grow larger. Alternatively, the pour point depressant might encourage
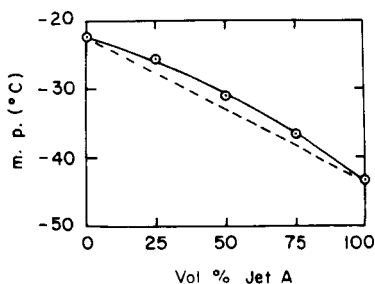
Fig. 6. DSC m.p. vs. vol.% X090-204 (Jet A) for fuels of Fig. 5.

nucleation of a different wax crystal structure. This latter explanation cannot be correct, however, since the m.p.s of fuels 7 and LFP-5 are identical within experimental error and the melting endotherms very similar. If the pour point depressant acts by lowering liquid-crystal surface tensions, one might expect it to affect the f.p., i.e. the degree of supercooling. However, comparison of the f.p.s of fuels 7 and LFP-5 shows no pronounced differences.

ACKNOWLEDGEMENT

REFERENCES

1 R. Friedman, ASME Paper No. 79-GT-141, March, 1979.
2 J.P. Longwell and J. Grobman, J. Eng. Power, 101 (1979) 155.
3 J. Solash, R.N. Hazlett, J.M. Hall and C.J. Nowack, Fuel, 57 (1978) 521.
4 F.J. Stockemer, Rep. No. CR-159615, NASA–Lewis Research Center, Cleveland, OH, 1979.
5 F. Noel, J. Inst. Pet. London, 57 (1971) 354.
6 F. Noel, Thermochim. Acta, 4 (1972) 377.
7 J.L. McNaughton and C.T. Mortimer, Differential Scanning Calorimetry, Perkin-Elmer Corp., Norwalk, CT, 1975.
8 F. Noel and G. Cranton, Am. Lab., June (1979) 27.
9 1974 Annual Book of ASTM Standards, Part 25, ASTM, Philadelphia, PA, p. 35.
10 1976 Annual Book of ASTM Standards, Part 24, ASTM, Philadelphia, PA, p. 336.
11 O.H. Wyatt and D. Dew-Hughes, Metals, Ceramics and Polymers, Cambridge University Press, London, 1974, p. 93, or other text on physical chemistry or materials science.
12 J.G. Zimmerman, Rep. No. 77-0049, David W. Taylor Naval Ship R & D Center, Bethesda, MD, May, 1977.
13 R.H. Doremus, Glass Science, Wiley, New York, 1973, Chaps. 2 and 5.
14 E. Dimitroff, J.T. Gray, Jr., N.T. Meckel and R.D. Quillian, Jr., Seventh World Petroleum Congress Proceedings, Vol. VIII, Part 2, Elsevier, New York, 1967, p. 141.
15 D.R. Uhlmann, G. Kritchevsky, R. Straff and G. Scherer, J. Chem. Phys., 62 (1975) 4896.
16 H.L. Finke, M.E. Gross, G. Waddington and H.M. Huffman, J. Am. Chem. Soc., 76 (1954) 333.
17 C.T. Moynihan and T. Bardakci, unpublished calculation.
18 G.A. Holder and J. Winkler, J. Inst. Pet. London, 51 (1965) 228.
19 B. Wunderlich, Thermochim. Acta, 5 (1973) 369.